Anisotropy and temperature dependence of electric-dipole resonances at dislocations in *p*-Si

V. V. Kveder and T. R. Mchedlidze

Institute of Solid-State Physics, Russian Academy of Sciences
(Submitted 29 November 1991)
Zh. Eksp. Teor. Fiz. **102**, 174–186 (July 1992)

We investigate the anisotropy and temperature dependence of electric-dipole spin resonance (EDSR) in plastically deformed *p*-type silicon, and determine the parameters of the *g*-tensor for the four ground-state lines. We show that EDSR can be interpreted in terms of the resonance of holes in quasi-one-dimensional bands corresponding to the regular rectilinear portions of screw and 60° dislocations.

INTRODUCTION

Under ideal conditions, dislocations in Si (and in other semiconductors) are one-dimensional systems with very interesting electronic properties, among them the presence of associated one-dimensional energy bands. However, the cores of real dislocations usually contain a large number of specific defects, which give rise to associated localized electronic states whose electrical activity strongly masks the properties of regular dislocation segments.

To separate the effects due to regular dislocation segments from effects due to dislocation defects, it is first necessary to decrease the number of these defects, and secondly to use methods that are sensitive to the localization length of the electronic wave functions in the direction of the dislocation. The first goal can be achieved by using a special two-stage plastic deformation[1] which makes it possible to obtain long rectilinear dislocations. In Refs. 2 and 3 we showed that one promising method for investigating quasi-one-dimensional bands associated with regular segments of dislocation cores is electric-dipole spin resonance (EDSR).

The idea of EDSR is based on the following observation: when a system possesses sufficiently low symmetry, specifically it has no center of inversion, the spin-orbit interaction leads to the appearance of a term of the form $\mathbf{V}(\mathbf{pS})$ in the electron Hamiltonian,[4] where $\mathbf{p}$ is the electron momentum, $\mathbf{S}$ is its spin, and $\mathbf{V}$ is a constant having the dimensions of velocity. If the sample is placed in a high-frequency electric field E_ω with frequency ω, a component of momentum $\mathbf{p}_\omega$ appears at this frequency such that $\mathbf{p}_\omega = \mu_{ij}\mathbf{E}_\omega$, where μ is a complex tensor. When the electronic states are localized, μ is a measure of the polarization of the electronic system due to mixing of excited electronic states stimulated by the field $\mathbf{E}_\omega$, while for band states $\mathbf{p}_\omega/m$ corresponds to the drift velocity and μ has the sense of a high-frequency electron mobility in the band. The presence of the term $\mathbf{V}(\mathbf{pS})$ implies that the following effective magnetic field acts on the electron spin:

$$\mathbf{h}_\omega = \mathbf{V}(\mathbf{p}_\omega \mathbf{S})/g\mu_B,$$

where g and μ_B are the g-factor and Bohr magneton respectively. When an external magnetic field $H_0 = \hbar\omega/g\mu_B$ is applied, the field $\mathbf{h}_\omega$ will excite resonant transitions between the Zeeman levels, which should lead to the appearance of a strong resonance in the permittivity of the sample:

$$\varepsilon(\omega) = \varepsilon' + i\varepsilon''.$$

We will refer to this resonance as EDSR.

From the simple discussion presented here, it is clear that the EDSR intensity, which is proportional to $\mathbf{h}_\omega^2$, can be quite large if $(\mathbf{V}\mathbf{p}_\omega)^2$ is large. If the ground state is localized and the frequency ω is sufficiently low, the field $\mathbf{E}_\omega$ will mix the former with excited states, leading to a nonzero value of $\mathbf{p}_\omega$. This mixing will be large when the wave function in the direction of the field $\mathbf{E}_\omega$ has large (ideally, infinite) radius. Therefore, the electronic states that will be most visible in EDSR are those that are strongly localized in the direction perpendicular to the dislocations but delocalized along the dislocations. These requirements are best satisfied by electrons or holes in deep one-dimensional bands associated with regular segments of the dislocation cores (if such bands exist).

The authors of Ref. 5 reported that they had observed a previously unknown EDSR spectrum in *p*-Si crystals containing rectilinear dislocations. Low-temperature annealing of their samples, which resulted in warping of the dislocations without changing their density, led to disappearance of the EDSR signal. This fact argues strongly in favor of the idea that the observed EDSR spectrum could be associated with regular dislocation segments. The goal of this paper is to investigate the anisotropy of the temperature dependence of this EDSR.

SAMPLES AND THEIR METHOD OF PREPARATION

We used single-crystal silicon doped with donors at a concentration of $4\cdot10^{15}$ at. cm^3. Rectangular samples with dimensions $10\times4\times3.5$ mm^3 were plastically deformed by compressing them along the long axis of the sample, which corresponded to a crystallographic direction that is rotated around [1, − 1,0] until it deviates by 10° from [110]. This geometry ensured that the plastic deformation due to the motion of dislocations occurred primarily in one plane (111). In order to generate rectilinear dislocations with a small number of kinks, we used a two-stage plastic deformation (see Ref. 1):

(1) A deformation of 1.5 to 2% at 700 °C under a load of 100 MPa (which corresponds to dislocation densities of $3\cdot10^8$ to 10^9 cm^{-3}).

(2) A 90-minute anneal at 900 °C to decrease the con-

 0038-5646/92/070092-07$05.00

centration of broken bonds and point defects.

(3) A second deformation at 410 °C under a load of 330 MPa for 90 minutes with cooling under load.

This last procedure transforms the dislocations introduced previously into rectilinear segments of screw and 60° dislocations directed along $[-1,0,1]$, $[0,-1,1]$, and $[1,-1,0]$. In this case, each dislocation has either $[-1,0,1]$ or $[0,-1,1]$ as its Burgers vector. We then cut out layers with dimensions $3\times3\times0.3$ mm^3 from the central portion of the sample, and made our measurements on these layers. The thickness of the layers was chosen to be smaller than a skin depth.

To record the EDSR, the samples were placed in the rectangular (H 102) cavity of a superheterodyne X-band EPR spectrometer and subjected to a cavity electric field $\mathbf{E}_\omega$. The samples were positioned such that $\mathbf{E}_\omega$ lay in the plane of the sample. The static magnetic field H_0 was modulated at a frequency of 80 Hz and an amplitude of 8 Oe, which allowed us to record the spectrum of $\partial\varepsilon''(H_0)/\partial H_0$, where ε'' is the imaginary part of the permittivity of the sample, which corresponds to absorption of microwave power. Because the sample had to be screened from nonuniform IR illumination, we monitored the illumination of the sample in the resonator by placing a miniature incandescent lamp in the latter.

At a point in the cavity where H_ω was a maximum we glued on standard paramagnetic sample ($CuSO_4\cdot5H_2O$), and divided the EDSR spectrum by the amplitude of the signal from the EPR standard. This was necessary in order to take into account the change in the Q-factor of the cavity as the sample was rotated and as the temperature varied (the samples we used possessed large anisotropy in their microwave conductivity due to the dislocations).

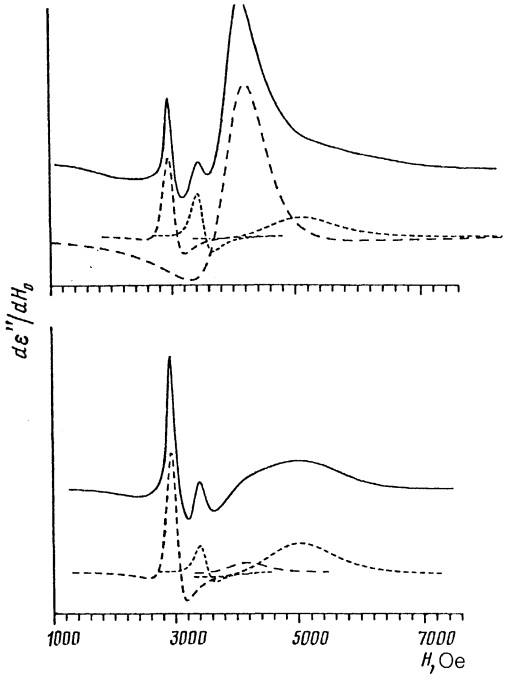

FIG. 1. EDSR spectrum obtained at 1.4 K as the sample was rotated around the axis $\Omega = [111]$ (here the axis Ω is perpendicular to $\mathbf{H}_0$ and $\mathbf{E}_\omega$); $\mathbf{H}_0$ makes an angle of 140° with the $[1,-1,0]$ axis. The lower spectrum corresponds to the geometry $\mathbf{H}_0\|\mathbf{E}_\omega$, the upper to $\mathbf{H}_0\perp\mathbf{E}_\omega$.

ANISOTROPY OF THE ELECTRIC-DIPOLE SPIN RESONANCE

To study the anisotropy of the EDSR spectra, we rotated the samples around three axes $\Omega = [111]$, $[1,1,-2]$, and $[1,-1,0]$ and measured the dependence of the spectra on the rotation angles. In this case, the vectors $\mathbf{H}_0$ and $\mathbf{E}_\omega$ were perpendicular to Ω and each series was plotted in two geometries: (a) $\mathbf{E}_\omega\|\mathbf{H}_0$, and (b) $-\mathbf{E}_\omega\perp\mathbf{H}_0$. All measurements were made at $T = 1.4$ K, and at microwave powers on the order of 10^{-6} W.

Illumination of the sample by white light led to some increase in the resolution of the spectrum due to the increased amplitudes of the individual spectral lines and a decrease in their widths. For this reason, the anisotropy was measured with a small bias illumination.

In Fig. 1, we show as an example EDSR spectra obtained for the same sample orientation with respect to $\mathbf{H}_0$. The lower spectrum corresponds to geometry "a" (i.e., $\mathbf{H}_0\|\mathbf{E}_\omega$), while the upper is in the "b" geometry ($\mathbf{H}_0\perp\mathbf{E}_\omega$). Under each spectrum we show its resolution into individual lines). Although the spectrometer was adjusted to record the absorption spectrum, and the EPR signal from the paramagnetic etalon is a pure absorption line, the EDSR line shape did not correspond to the absorption curve, but rather was a mixture of the absorption and dispersion curves. An analogous absorption line shape was observed in Ref. 2 for EDSR of electrons in a deep one-dimensional band (the *Ch* line) and was attributed to polarization effects due to finite-length conducting dislocation segments (i.e., to finite localization length of the electrons in the one-dimensional band). We will return to the question "what is the line shape?" in the discussion of results.

It is clear from Fig. 1 that the resolution of the spectrum is not very good; therefore, in order to analyze the anisotropy of the g-factors and amplitudes of the lines, we used a computer to resolve the spectrum into individual lines by the method of least squares. The authors of Ref. 5 used their observations of the two-photon EDSR spectrum to show that the resonance magnetic field is proportional to frequency, indicating that a simple spin Hamiltonian can be used: $H = \mu_B g_{ij} S_i H_{0j}$.

In Fig. 2 we show data on the angular dependence of the g-factors of the lines as the sample was rotated around the three different axes. In the samples we investigated, six lines were observed at certain orientations; however, only analysis of the four most intense lines of the spectrum was possible. The lines for which the parameters of the g-factor were determined are labeled *1*, *2*, *4*, and *5* in Fig. 1. They can be grouped into two pairs: lines *4* and *5* have half-widths of 400 to 1100 Oe, and are well-described by a g-tensor with the principal values

$$g_{xx}\approx1{,}27\mp0{,}03,\quad g_{yy}\approx2{,}19\mp0{,}02,\quad g_{zz}\approx1{,}10\mp0{,}05$$

and principal axes

$X=[1,0,-1]$ and $Y=[010]$ — for line *4*
$X=[0,-1,1]$ and $Y=[100]$ — for line *5*.

For definiteness we will refer to the centers corresponding to these lines as Si–*KC* 1.

Lines *1* and *2* have half-widths of order 90–160 Oe and

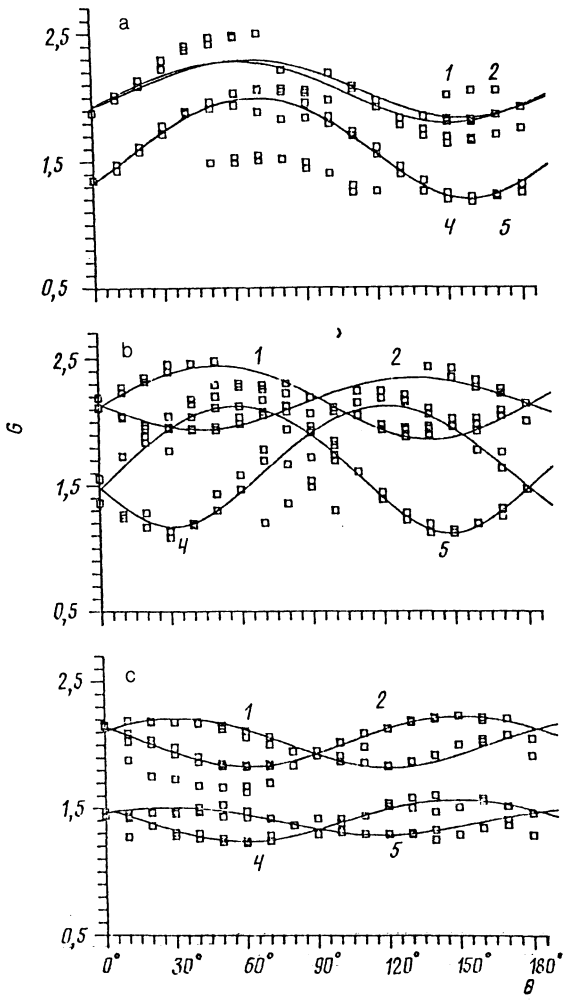

FIG. 2. Dependences of the line g-factors on the angle θ between $\mathbf{H}_0$ and the axis [1, − 1,0] (for Figs. 2b and 2c) or the axis [1,1, − 2] (for Fig. 2a). The axes of rotation are $\Omega = [1, -1,0]$, $[1,1, -2]$ and $[111]$ for a, b, and c, respectively.

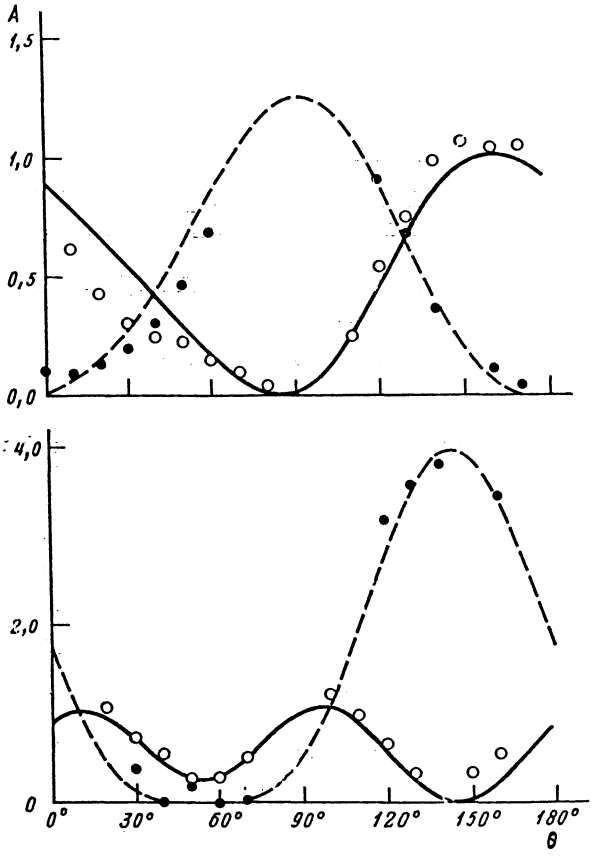

FIG. 3. Dependence of the amplitude of line 4 on the angle between $\mathbf{H}_0$ and the axis [1, − 1,0]. The lower figure is for a rotation around $\Omega = [111]$, the upper is for a rotation around $\Omega = [1,1, -2]$; O is for geometry "a" ($\mathbf{H}_0 \| \mathbf{E}_\omega$) and ● is for geometry "b" ($\mathbf{H}_0 \perp \mathbf{E}_\omega$).

can be described by the g-tensor with principal values

$$g_{xx} \approx 1{,}82 \mp 0.02, \quad g_{yy} \approx 2{,}48 \mp 0.04, \quad g_{zz} \approx 1.89 \mp 0{,}03$$

and principal axes

$X = [0, -1,1]$, $Y = [100]$ for line *1*,
$X = [1,0, -1]$, $Y = [010]$ for line *2*.

We will call the centers corresponding to these lines Si–*KC* 2.

The amplitudes of the lines depend strongly on the orientation of the sample and the angle between $\mathbf{H}_0$ and $\mathbf{E}_\omega$. In Fig. 3, we show as an example the anisotropy of the amplitude of line *4* as the sample was rotated around the axes $\Omega = [111]$ and $\Omega = [1,1, -2]$. We attempted to describe the anisotropy of the line amplitudes using the assumption that the hole wave functions were quasi-one-dimensional, i.e., assuming that the spin transitions are caused only by the component of $\mathbf{E}_\omega$ along the vector $\mathbf{L}$ corresponding to the long axis of the wave function. In this case, the orientation of the effective magnetic field $\mathbf{h}_\omega$, which perturbs the spin through the spin-orbit interaction, does not depend on the direction of the field $\mathbf{E}_\omega$, and the amplitude of the line is given by the simple expression

$$A = A_0 (\mathbf{L}\mathbf{E}_\omega)^2 [\mathbf{h}_\omega \mathbf{H}_0]^2 / h_\omega^2. \qquad (1)$$

Despite the rather low accuracy of our measurements of the line amplitudes, owing to their strong overlap, as well as the fact that the spin states of the hole are not pure $S = 1/2$ states, we obtained rather good agreement with experiment by using Eq. (1). From a comparison of the experimental functions with Eq. (1), we obtain the following parameters:

Line *1*: $A_0 = 2{,}8$; $\mathbf{L} = [1, -1,0] \mp 7°$; $\mathbf{h}_\omega = [101] \mp 10°$,
Line *2*: $A_0 = 4{,}2$; $\mathbf{L} = [1, -1,0] \mp 7°$; $\mathbf{h}_\omega = [011] \mp 10°$.
Line *4*: $A_0 = 3{,}2$, $\mathbf{L} = [1,0, -1] \mp 5°$; $\mathbf{h}_\omega = [2,0, -1] \mp 7°$
Line *5*: $A_0 = 2{,}7$; $\mathbf{L} = [0, -1,1] \mp 5°$; $\mathbf{h}_\omega = [0, -1,2] \mp 7°$.

TEMPERATURE DEPENDENCES

To measure the temperature dependences we chose an orientation of the sample for which lines *2* and *4* dominated in the spectrum and were rather well resolved, and used the geometry $\mathbf{E}_\omega \perp \mathbf{H}_0$. As we mentioned above, the EDSR spectrum was normalized by the EPR signal from the paramagnetic standard.

In Fig. 4, we show the temperature dependences of the amplitudes of lines *2* and *4* obtained before and during illumination of the sample by light corresponding to black-body radiation with a maximum in the region 2 μm. After switching off the light, we observed a slow relaxation of the spectrum to its dark value, with two strongly differing character-

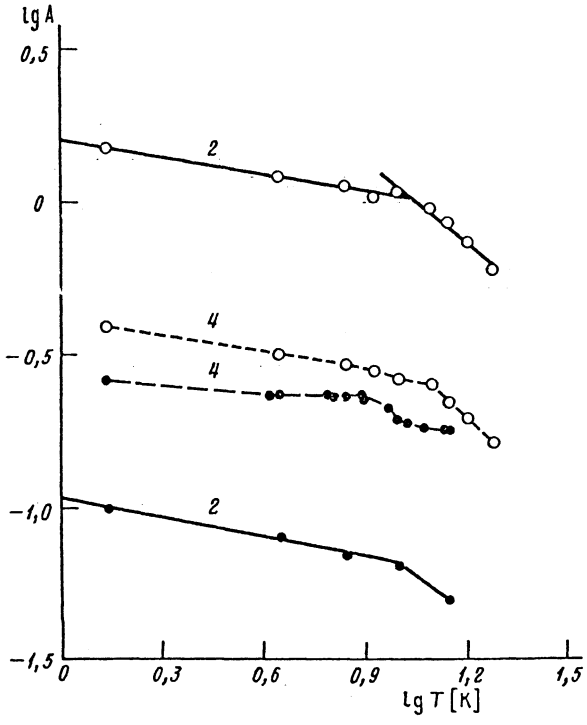

FIG. 4. Temperature dependence of the EDSR amplitude normalized by the EPR of the paramagnetic standard: ● was measured before illumination for the sample, ○ during illumination.

istic times. In the temperature region 1.4 K to 20 K, these times are rather long (several minutes); therefore, the very low light intensity we used was "saturating," and the parameters of the line changed very little even when the intensity of the light changed by factors of 2 to 3.

As the field E_ω (i.e., the microwave power) increased, we observed saturation of the amplitude A of the $\partial\varepsilon''/\partial H_0$ line. The dependence of A on E_ω is well-described by the expression

$$A=A_0/(1+\alpha E_\omega^2)^{1/2}, \tag{2}$$

which is characteristic of inhomogeneously broadened lines. here $\alpha = 4\pi^2\gamma^2K^2\tau_1\tau_2$, where γ is the gyromagnetic ratio, τ_1 and τ_2 are the spin-lattice and spin-spin relaxation times, and $K = |h_\omega|/|\mathbf{L}\cdot\mathbf{E}_\omega)|$ is a coefficient of proportionality between the microwave field $\mathbf{E}_\omega$ and the effective magnetic field $\mathbf{h}_\omega$.

DISCUSSION OF RESULTS

As we mentioned above, the EDSR line has an unusual shape corresponding to a mixture of dispersion and absorption. Furthermore, the anisotropy of the amplitude of the line is described satisfactorily by a model which assumes that the wave functions are quasi-one-dimensional. These facts argue in favor of the idea that we should try to interpret at least a part of the observed line as EDSR of quasi-one-dimensional holes in the dislocation potential. This problem was solved theoretically in Refs. 2 and 6.

Let us assume that a hole trapped in a dislocation potential is free to move along a finite rectilinear dislocation segment of length L, and that its high-frequency mobility in this quasi-one-dimensional potential is $\mu(\omega)$. Then the high-frequency conductivity of the sample

$$\sigma(\omega)=\omega\varepsilon''(\omega)/4\pi$$

due to these dislocation segments for $E_\omega \| L$ and $h_\omega \perp H_0$ is given by the expression

$$\sigma(\omega)/L_t = eN\mu(\omega)S(L/L_D) - i\frac{N(\mu(\omega)S(L/L_D)mV)^2\Omega^2}{8kT(\omega-\Omega+i/\tau_2+iD(mV)_2S(L/L_s)/2(1-i\omega\tau))}, \tag{3}$$

where

$$S(x)=1-\exp(i\pi/4)\operatorname{tg}(x\exp(-i\pi/4))/x$$

is a structure factor, L_t is the total length of the conducting dislocation segments in the volume of the sample, N is the density of holes per unit length of the dislocation segment, $D = T\tau/m$ is the diffusion coefficient of holes along the segment, $L_s = (D/\omega)^{1/2}$, Ω is the spin resonance frequency, and

$$L_D=[(D+e\mu(\omega)N\ln(L^2/b^2)/\varepsilon)/\omega]^{1/2},$$

where b is the localization length transverse to the dislocation.

If we neglect the diffusion coefficient D in the expression for L_D, which should be small at low temperatures, Eq. (3) simplifies, and the list of fitting parameters is reduced to the following: the linewidth ΔH, the resonance field H_r, the "intensity" of the line $I = NL_t[\mu(\omega)V]^2$ (normalized by the paramagnetic standard), and the ratio

$$L/L_D \approx L/(e\mu(\omega)N\ln(L^2/b^2))^{-1/2}.$$

These four parameters are determined for each temperature by minimizing the mean-square difference between the experimental and calculated spectra.

In Fig. 5 we show the temperature dependences obtained in this way for the quantity $I^{1/2}=\mu(\omega)V(NL_t)^{1/2}$ for lines *2* and *4*. Here NL_t has the sense of the total number of holes that contribute to this EDSR line.

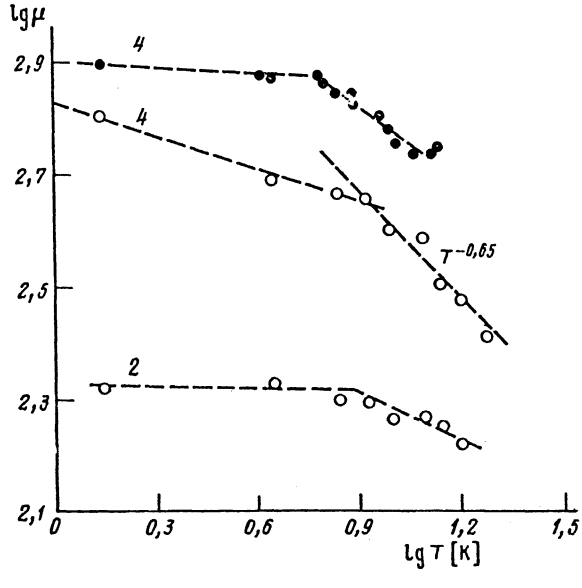

FIG. 5. Temperature dependence of the quantity $I^{1/2}=\mu(\omega)VN_t^{1/2}$ for lines *2* and *4*: ● was measured before illumination of the sample, ○ during illumination.

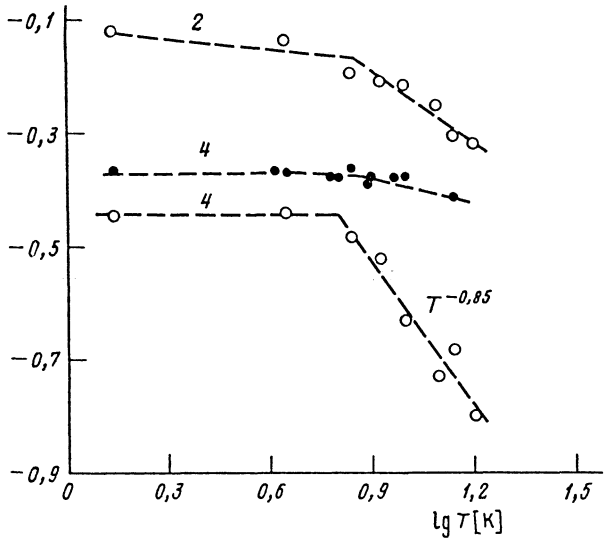

FIG. 6. Temperature dependence of the quantity $c\mu(\omega)N/L^2$ for lines *2* and *4*: ● was measured before illumination of the sample, O during illumination.

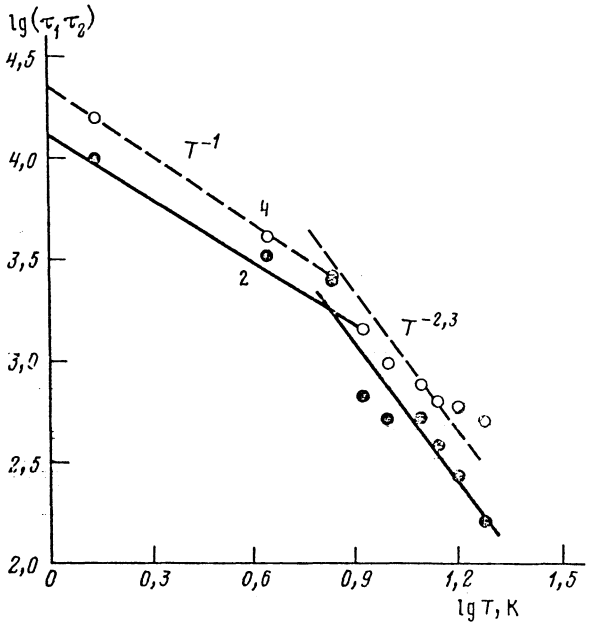

FIG. 7. Temperature dependence of the quantity $\alpha/A_0 \propto \tau_1\tau_2$ (in arbitrary units) for line *2* (●) and line *4* (O) during illumination.

The line shape (which reflects the degree to which the dispersive part is mixed in) is determined by the complex structure factor $S(L/L_D)$. Therefore, by analyzing the line shape we can determine the quantity $c\mu(\omega)N/L^2 = (L/L_D)^{-2}$ independently of the line amplitude, where $c = e\ln(L^2/b^2)$ is a slowly-varying quantity. The dependence of $c\mu(\omega)N/L^2$ on temperature is shown in Fig. 6.

We can assume that the number of holes trapped in dislocation states corresponding to the Si–*KC* 1 and Si–*KC* 2 centers does not depend on temperature, at least for $T<20$ K. This implies that in the temperature interval under discussion we have $NL_t = \text{const}$. We can also assume that at low temperatures V does not depend on T. Then Fig. 5 corresponds to the temperature dependence of $\mu(\omega)$, while Fig. 6 is the temperature dependence of the quantity $\mu(\omega)/L^2$. Comparing Figs. 5 and 6, we see that the temperature dependences obtained for the quantities $\mu(\omega)$ are close to those of the quantities $\mu(\omega)/L^2$. The small differences in the slopes can be attributed to an increase in the localization length L as the temperature increases. The satisfactory agreement between the functions in Figs. 5 and 6 is an argument in favor of the validity of Eq. (3) in our case.

Since the amplitude of line *A* multiplied by the square of its half-width ΔH is proportional to the constant K^2, where the "field enhancement" coefficient is

$$K=|h_\omega|/|(\mathbf{LE}_\omega)|=\mu(\omega)S(L/L_D)emV/\mu_B,$$

division of the saturation factor α by $A(\Delta H)^2$ should yield a quantity proportional to $\tau_1\tau_2$. In Fig. 7 we show the temperature dependences of $\tau_1\tau_2$ obtained in this way. Assuming that $\tau_2 = \text{const}$ for $T<8$ K, we have $\tau_1 \sim T^{-1}$, which is characteristic of the one-phonon relaxation processes that dominate at low temperatures. For $T>8$ K we have $\tau_1 \sim T^{-2.3}$, at which point the two-phonon processes apparently begin to dominate. It is well known that for two-phonon processes we should expect a stronger temperature dependence (proportional to T^{-5} up to T^{-7}). However, for dislocation centers one usually observes dependences with exponents between 2 and 3 for *Ch*-centers (Ref. 2) and *D*-centers (Refs. 7, 8). This can be explained by the dominant contribution of quasilocal vibrational modes of the dislocation to the spin-lattice relaxation (see Ref. 9).

Within the framework of one-dimensional band models, we can analyze how the influence of weak IR illumination on the sample should reveal itself. Let us see how the characteristic parameters of the Si–*KC* 1 centers change (line *4*) when the light is turned on: at 4.5 K the line width ΔH decreases by a factor of 1.3, the quantity (L/L_D) in the square root of the line intensity $(I)^{1/2}$ decreases by 1.4 times, and the saturation factor α increases by a factor of 3. This means that

$$\mu n^{1/3}/\mu_* n_*^{1/3}=1{,}4,\ \mu(\tau_1\tau_2)^{1/3}/\mu_*(\tau_1\tau_2)_*^{1/3}=0{,}64,\ \mu L^2/\mu_* L_*^2=1{,}4,$$

where the asterisks in the subscripts denote the presence of illumination, and n is the total number of holes in the states corresponding to Si–*KC* 1 centers. Usually the quantity τ_1 decreases when the sample is illuminated, owing to the exchange interaction with the free carriers, i.e., $\tau_1 > \tau_{1*}$. Analysis of the change in line width during saturation shows that before illumination the inhomogeneous part of the line broadening is $\Delta H_n \approx 730$ Oe and the homogeneous part is $\Delta H_u = 1/\tau_2 \approx 250$ Oe. During illumination we have $\Delta H_n \approx 300$ Oe, $\Delta H_u \approx 1/\tau_2 \approx 400$ Oe, i.e., τ_2 decreases under illumination. Although the accuracy of these estimates is not very great, it is clear that $(\tau_1\tau_2) > (\tau_1\tau_2)_*$. Even assuming that $(\tau_1\tau_2) = (\tau_1\tau_2)_*$, we have $\mu/\mu_* < 0.6$, implying that $L/L_* < 0.7$, $n/n_* > 4$.

This shows that under illumination there is a strong decrease in the number of holes trapped at Si–*KC* 1 centers, and that their mobilities and localization lengths increase. This can be explained by the fact that optical excitation causes not only a decrease in the number of holes trapped on the Si–*KC* 1 centers, but also a decrease in the number of holes held in more deeply localized states caused by the various defects that are present in the dislocation cores, in par-

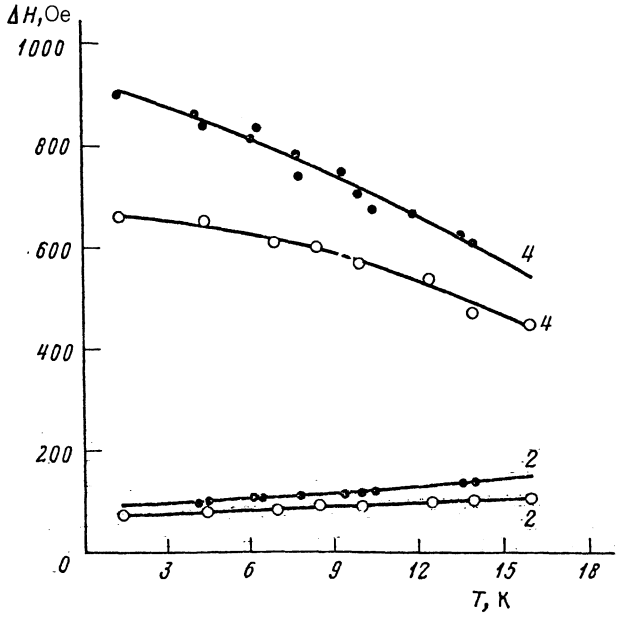

FIG. 8. Temperature dependence of the half-widths of lines *2* and *4*: ●—before illumination, ○—during illumination.

ticular, the rather small number of broken bonds that remain despite our annealing of the samples. The latter lead to a decrease in the random potential caused by localization of the quasi-one-dimensional holes, and hence to an increase in μ and L. The holes that are activated by light are trapped at boron atoms.

Analogous estimates for Si–*KC*2 centers (line *2*), although less accurate, show that illumination does not change the number of holes trapped at these centers very much, and that the strong growth in the amplitude of the lines under illumination is due to the linewidth decrease (by a factor of 1.3), by some increase in the mobility (by a factor of 1 to 1.2), and by a considerable increase in the localization length (by a factor of 1.5).

The increase of L under illumination of the sample correlates with the observed decrease in the inhomogeneous line width (see Fig. 8). In fact, as L increases the nonuniform fields of the various defects acting on a hole should become more effectively averaged.

Comparing the intensities of lines *2* and *4* with the EPR signal of the standard, we have for line *2* at $T = 4.5$ K

$$K^2NL_t = 8\cdot 10^{24}\ \text{cm}^{-3}$$

or

$$(K/S(L/L_D))^2NL_t = 5\cdot 10^{25}\ \text{cm}^{-3}.$$

For line *4* we have

$$K^2NL_t = 1\cdot 10^{26}\ \text{cm}^{-3}$$

or

$$(K/S(L/L_D))^2NL_t = 2{,}4\cdot 10^{26}\ \text{cm}^{-3}.$$

Since NL_t cannot exceed the concentration of boron atoms, taking as a lower estimate of K the value $NL_t = 10^{15}\ \text{cm}^{-3}$, for line *2* we have $K > 10^5$ and

$$K/|S(L/L_D)| = \mu(\omega)emV/\mu_B > 5\cdot 10^5,$$

while for line *4* we have accordingly $K > 5\cdot 10^5$ and

$$\mu(\omega)emV/\mu_B > 10^6.$$

Such enormous values for K can be explained by the large value of the spin-orbit interaction for holes in silicon under the additional conditions of rather large localization lengths L for holes along the dislocation, i.e., the presence of quasi-one-dimensional bands. The fact that μ decreases as the temperature increases agrees with this concept, and can be interpreted in terms of scattering of the one-dimensional holes by phonons.

Thus, the results we have obtained for lines *4* and *5* correlate well with a model of one-dimensional dislocation bands. As for the other lines, our data on them also do not contradict this model; however, for an unambiguous conclusion additional investigations would be desirable.

Let us now discuss our anisotropy results. The fundamental vectors that define a dislocation are the direction of the dislocation line **L** and its Burgers vector **b**. As we mentioned above, in this sample there are dislocations with two Burgers vectors: $[-1,0,1]$ and $[0,-1,1]$. This implies that the dominant slip system contains six dislocation groups, namely: two screw dislocation groups, $\mathbf{L} = [-1,0,1]$, $\mathbf{b} = [-1,0,1]$ and $\mathbf{L} = [0,-1,1]$, $\mathbf{b} = [0,-1,1]$, and four 60° dislocation groups: $\mathbf{L} = [-1,0,1]$, $\mathbf{b} = [0,-1,1]$; $\mathbf{L} = [0,-1,1]$, $\mathbf{b} = [-1,0,1]$; $\mathbf{L} = [1,-1,0]$, $\mathbf{b} = [-1,0,1]$; and $\mathbf{L} = [1,-1,0]$, $\mathbf{b} = [0,-1,1]$. Furthermore, we must also take into account that the complete dislocations we mentioned above can be resolved into partial ones (as is well known, a screw dislocation resolves into three 30° parts, while a full 60° dislocation resolves into a 30° and 90° part). Accordingly, if we associate the observed EDSR signal with the regular portions of dislocation cores, in general we should expect the presence of six lines.

The main contribution to the integrated EDSR intensity of the spectrum is made by the two broad lines 4 and 5. Starting from the data on the anisotropy of the amplitude of these lines, we can conclude that lines *4* and *5* correspond to dislocations with $\mathbf{L} = [-1,0,1]$ and $\mathbf{L} = [0,-1,1]$. In this case, the X-axes of their g-tensors coincide with **L**. It is very probable that lines *4* and *5* correspond to one-dimensional bands caused by screw dislocation segments.

As for the less intense lines *1* and *2*, the anisotropy of their amplitudes is well described by assuming that both correspond to $\mathbf{L} = [1,-1,0]$, whereas the axes of the g-tensor lie in the directions $\mathbf{X} = [0,-1,1]$ and $\mathbf{Y} = [100]$ for line *1* and $\mathbf{X} = [1,0,-1]$ and $\mathbf{Y} = [010]$ for line *2*. It is possible that these lines are due to 60° dislocations lying in the direction $[1,-1,0]$, and that the anisotropy of the g-factor is controlled by their Burgers vectors. In this case, the following question remains: why were the EDSR amplitudes from the other two 60° dislocation groups so small that we were unable to detect them for any orientation? One possible answer is the following: these dislocations differ from $[1,-1,0]$ by the ordering of the components of their partial dislocations, which can affect the degree of their defectiveness and consequently the value of L on which the EDSR intensity depends strongly. Furthermore, they are parallel to the screw dislocations and possess high conductivity, lead-

ing to local distortion (shunting) of and the field $\mathbf{E}_\omega$ and suppression of EDSR from dislocations lying near the 60° dislocations. However, no final conclusion can be drawn without additional experiments.

[1] K. Wessel and H. Alexander, Phil. Mag. **35**, 1523 (1977).
[2] V. V. Kveder, A. E. Koshelev, T. R. Mchedlidze, *et al.*, Zh. Eksp. Teor. Fiz. **95**, 183 (1989) [Sov. Phys. JETP **68**, 104 (1989)].
[3] V. V. Kveder, T. R. Mchedlidze, Yu. A. Osipyan, and A. I. Shalynin, in *Defect Control in Semiconductors*, K. Sumino (ed.), Elsevier Sci. Publ. B. V. (North-Holland), 1990, p. 1417.
[4] E. I. Rashba, Fiz. Tverd. Tela **2**, 1224 (1959) [Sov. Phys. Solid State **2**, 1109 (1960)].
[5] M. Wattenbach, C. Kisielowski-Kemmerich, H. Alexander, Phys. Status Solidi (b) **158**, K49 (1990).
[6] A. E. Koshelev, V. Ya. Kravchenko, and D. E. Khmel'nitskiĭ, Fiz. Tverd. Tela **30**, 433 (1988) [Sov. Phys. Solid State **30**, 246 (1988)].
[7] V. A. Grazhulis, V. V. Kveder, and Yu. A. Osipyan, Phys. Status Solidi (b) **103**, 549 (1981).
[8] C. Kisielowski-Kemmerich, G. Weber, and H. Alexander, Proc. 13th ICDS, Coronado, 1984.
[9] V. M. Vinokur and V. Ya. Kravchenko, Pis'ma Zh. Eksp. Teor. Fiz. **29**, 626 (1979) [JETP Lett. **29**, 572 (1979)].

Translated by Frank J. Crowne